Eur Radiol
DOI 10.1007/s00330-013-3005-9

NEURO

The common dementias: a pictorial review

Pervinder Bhogal · Colin Mahoney · Sophie Graeme-Baker · Amit Roy · Sachit Shah · Francesco Fraioli · Peter Cowley · Hans Rolf Jäger

Received: 17 April 2013 / Revised: 8 August 2013 / Accepted: 9 August 2013

Abstract Imaging plays an important role in the diagnosis and management of dementia. This review covers the imaging features of the most common dementing illnesses: Alzheimer's disease (AD), vascular dementia (VaD), dementia with Lewy bodies (DLB) and frontotemporal lobar degeneration (FTLD). It describes typical findings on structural neuroimaging and discusses functional and molecular imaging techniques such as FDG PET, amyloid PET, magnetic resonance (MR) perfusion imaging, diffusion tensor imaging (DTI) and functional MR imaging (fMRI).

Keywords Imaging · Dementia · Alzheimer's · Frontotemporal · Lewy bodies

Introduction

Imaging plays an important role in the diagnosis and management of dementia. This review covers the imaging features of the most common dementing illnesses: Alzheimer's disease (AD), vascular dementia (VaD), dementia with Lewy bodies (DLB) and frontotemporal lobar degeneration (FTLD).

The standard structural magnetic resonance imaging (MRI) protocol for dementia should include the following sequences: three-dimensional T1-weighted gradient echo with 1-mm isotropic voxels, axial T2-weighted fast spin echo, coronal or axial fluid-attenuated inversion recovery (FLAIR), diffusion weighted images (DWI) and a haemorrhage-sensitive sequence (either T2*-weighted or susceptibility-weighted). A structured approach to reporting these images [1] is helpful and should consider: (1) surgically treatable lesions such as a mass lesion, subdural haematoma or hydrocephalus; (2) presence, extent and location of small and large vessel disease; (3) presence and distribution of cerebral micro bleeds; (4) degree and pattern of general cortical atrophy; (5) focal atrophy with particular attention to the hippocampi, temporal lobes, precuneus, frontal lobes, midbrain and pons.

Of the advanced imaging methods, ^{18}F-fluorodeoxyglucose (FDG) positron emission tomography (PET) and amyloid PET are increasingly used in clinical practice, particularly at an early stage of the disease. More recently, advanced MR imaging techniques such as arterial spin labelling (ASL), DTI and fMRI have emerged as candidate imaging biomarkers in a range of neurodegenerative conditions. These techniques allow in vivo assessment of functional and structural brain networks and may offer improved ability to detect and monitor neurodegenerative conditions.

Alzheimer's disease

Alzheimer's disease (AD) is the most common cause of dementia and was originally described by Alois Alzheimer in 1906.

The pathological hallmarks of AD are two abnormal protein aggregates: amyloid plaques and neurofibrillary tangles [2–6]. Amyloid plaques are extracellular beta-amyloid surrounded by inflammatory cells; neurofibrillary tangles are intracellular aggregates of pathological tau protein.

P. Bhogal (✉) · S. Graeme-Baker · A. Roy · S. Shah · P. Cowley
Lysholm Department of Neuroradiology, National Hospital for Neurology and Neurosurgery, Queen Square, London WC1N 3BG, UK
e-mail: bhogalweb@aol.com

C. Mahoney
Dementia Research Centre, Department of Neurodegenerative Diseases UCL Institute of Neurology, London, UK

F. Fraioli
Institute of Nuclear Medicine, University College London, London, UK

H. R. Jäger
Neuroradiological Academic Unit, Department of Brain Repair and Rehabilitation, Lysholm Department of Neuroradiology, National Hospital for Neurology and Neurosurgery, UCL Institute of Neurology, Queen Square, Box 65, 8-11, London WC1N 3BG, UK

Published online: 01 October 2013

The disease typically presents with a progressive decline in episodic memory. Less frequently it may manifest with language or visual processing difficulties. Not uncommonly, multiple cognitive domains will become impaired with a global dementia emerging over time.

Most cases of AD are preceded by a period of mild cognitive impairment (MCI). This pre-dementia stage most commonly presents with impairment of episodic memory (amnestic MCI) with up 10–15 % of individuals progressing to dementia each year [7]. Some imaging features in MCI resemble those seen in AD; hippocampal atrophy being a particularly robust marker for predicting progression from MCI to AD [8].

Clinical diagnostic criteria for AD were defined in 1984. Recently the National Institute on Aging-Alzheimer's Association updated their diagnostic guidelines for AD, incorporating imaging and cerebrospinal fluid (CSF) biomarkers [9, 10]. They defined five major biomarkers, reflecting either an amyloid β accumulation (abnormal amyloid PET and low CSF levels of $A\beta_{42}$) or neuronal injury (elevated levels of CSF tau, decreased FDG uptake on PET, atrophy on structural MRI). A hypothetical model of evolution of AD biomarkers proposes markers of amyloid accumulation precede the onset of clinical symptoms by 15 or more years [11].

AD can be categorised into early and late onset, with 95 % of cases occurring after the age of 65 (late onset), with the incidence of AD doubling every 5 years after the age of 60 [12].

The ApoE e4 lipoprotein allele has been associated with an approximately 10–15 times increased risk for developing AD [1]. Autosomal dominant AD is rare and usually found in individuals with younger onset [13]. Three major genetic mutations have been identified that lead to familial AD: the amyloid precursor protein gene on chromosome 21; the presenilin 1 gene on chromosome 14 and the presenilin 2 gene on chromosome 1. All three mutations are involved in the metabolism of amyloid [14–19].

Cerebral volume loss is best assessed on high resolution volumetric T1-weighted MRI images. Focal volume loss classically starts in the entorhinal cortex, involves the medial temporal lobe and hippocampus, as well as medial parietal lobe [10]. Atrophy of the amygdala has also been recognised as a feature of AD [20]. A loss of volume in the region of 5 % per year has been reported in the hippocampus [21, 22]. In addition to focal atrophy, patients with AD also show more rapid global volume loss.

The degree of hippocampal atrophy correlates with clinical cognitive impairment [23–25].

The degree of medial temporal lobe atrophy (MTA) can be assessed using a five-point visual rating scale (ranging from 0 to 4) described by Scheltens et al. [26] (Fig. 1). Although mostly used for coronal T1 weighted MR images, this scale is also applicable to coronally reformatted CT images [27].

Ratings scales are very useful in a routine clinical setting and a dedicated centre may provide more advanced techniques of analysis. These include measurements of hippocampal volumes using either manual outlining or segmentation based approaches [28]. The assessment of volume changes over time is facilitated by spatial registration of serial T1-weighted volumetric images [1] and a diagnosis of AD can be corroborated if there is an appreciable hippocampal volume change within a 12- to 18-month interval (Fig. 2).

FDG-PET measures the glucose metabolism, which reflects predominantly synaptic activity. Hypometabolism on FDG PET can be detected before the onset of clinical symptoms, showing a typical topographic pattern: the posterior cingulate-precuneus region is affected first, followed by the lateral temporoparietal region (Fig. 3) [10, 11].

In addition, several PET tracers are now available for in vivo imaging of cerebral amyloid. The most extensively studied amyloid ligand is the Pittsburgh compound B (^{11}C -PIB). In patients with AD this tracer shows increased cortical uptake with the highest retention in the frontal, cingulated, precuneus, striatum, parietal and lateral temporal cortex (Fig. 4) [29]. Amyloid PET may also be potentially useful at detecting an underlying cause for MCI [30], but caution is required as abnormal tracer uptake is found in up to 30 % of cognitively normal elderly subjects [10]. Amyloid PET is therefore highly sensitive but not very specific for a diagnosis of AD. The use of

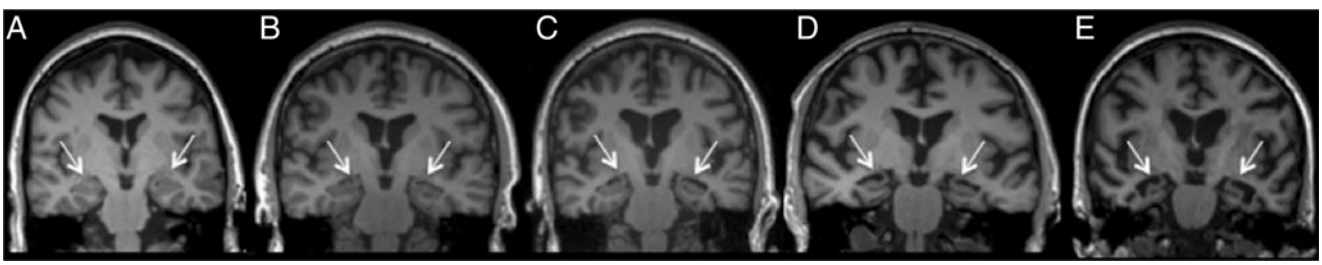

Fig. 1 Coronal T1-weighted MR images demonstrating different degrees of MTA. The visual rating scale incorporates the width of the choroid fissure, the width of the temporal horn and the height of the hippocampal formation. **a** Score 0—no atrophy. **b** Score 1—mild widening of the choroid fissure only. **c** Score 2—moderate widening of choroid fissure and temporal horn, with mild loss of hippocampal height. **d** Score 3—severe widening of choroid fissure and temporal horn, with moderate loss of hippocampal height. **e** Score 4—as for 3, but with severe loss of hippocampal height

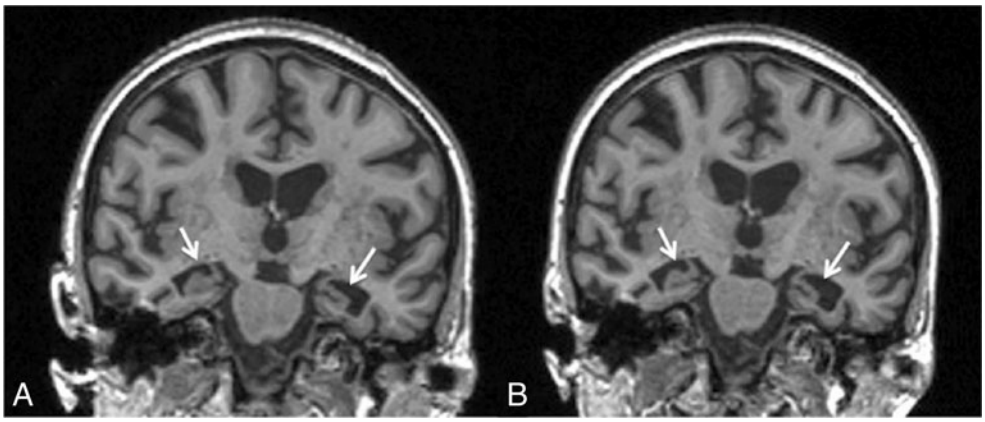

Fig. 2 Co-registered volumetric coronal T1-weighted images in a patient with AD, taken at baseline (**a**) and 12 months later (**b**) demonstrate clear volume loss of the hippocampi (*arrows*) and enlargement of the lateral ventricles with much less evident volume loss in the remainder of the brain

amyloid imaging for the diagnosis of dementia is likely to increase as fluorinated tracers become more widely available.

Amongst the advanced MR imaging techniques, perfusion imaging using arterial spin labelling (ASL), DTI and fMRI appear promising in dementia imaging. Regional hypoperfusion on ASL studies correlates well with hypometabolism on FDG PET [31] and the usefulness of ASL in diagnosing AD is becoming clear [32]. DTI measures microstructural change in white matter. Studies in AD have suggested that rather than being a focal process, white matter changes are distributed throughout the brain [33]. In particular, damage to limbic fibres such as the cingulum and fornix have been reported and changes here may provide greater specificity in the diagnosis of AD [34]. Functional MRI has been used to identify changes in resting state networks, with reduced activation of the default mode network most commonly reported [35]. Task-based fMRI utilising memory recall has also identified changes within limbic brain networks in individuals at higher risk of developing AD [36]. Whilst these techniques are not as yet readily used in clinical practice, preliminary studies suggest they may have a particular strength in determining the onset of disease and could be exploited as disease proximity biomarkers.

Posterior cortical atrophy

Posterior cortical atrophy (PCA) is characterised by a decline in functions that depend on posterior hemisphere structures. Patients typically present between 50 and 65 years of age with a decline in visuospatial and visuoperceptual skills, as well as problems with literacy and praxis, whilst memory and executive functions may be well preserved in the early stages of the disease. Pathological studies have shown that AD is the most common underlying cause of PCA [37, 38].

Structural imaging shows loss of volume in the occipital and parietal lobes with progressive involvement of the temporal lobes [39, 40]. A robust and reproducible rating scale for

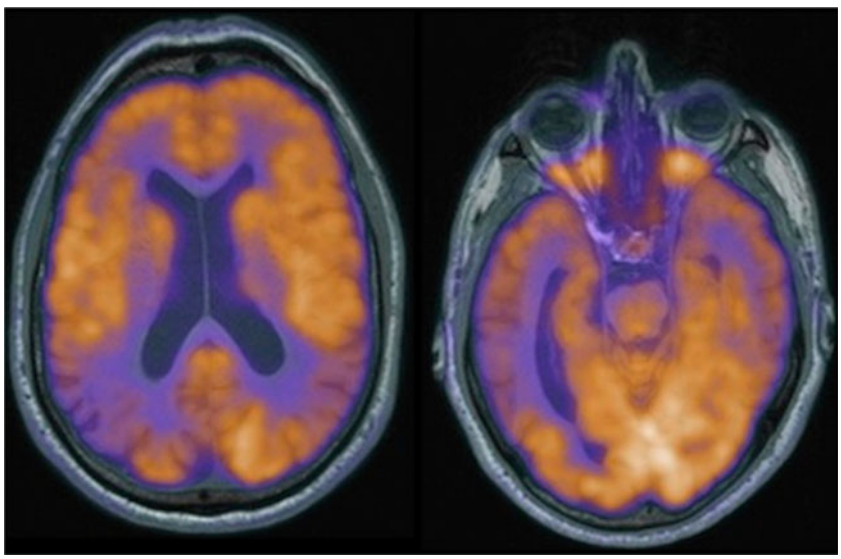

Fig. 3 FDG PET MRI in a patient with early AD demonstrating glucose hypometabolism in the parietal and temporal lobes. The lateral part of the temporal lobes is more severely affected than the medial part, which is a typical FDG PET finding of AD and distinct from the temporal lobe atrophy which is more prominent medially

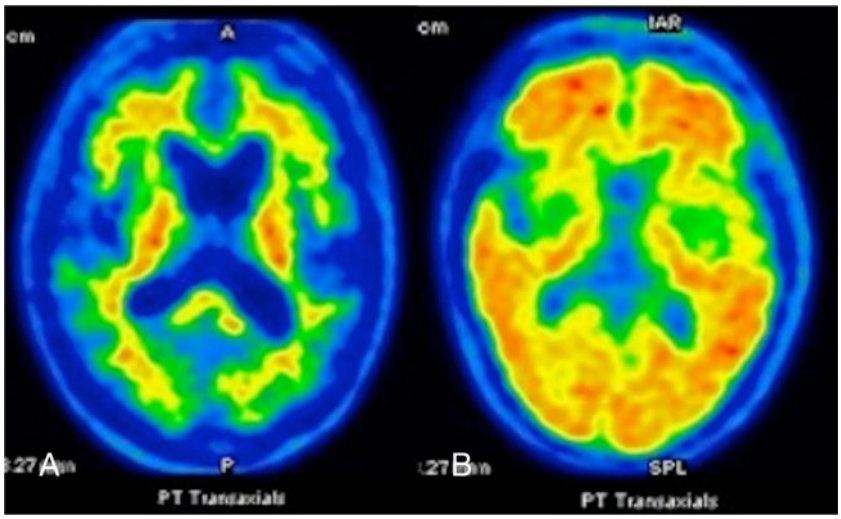

Fig. 4 Axial images of an amyloid PET CT using the tracer ^{11}C-PIB in a patient with progressive supranuclear palsy (PSP) (**a**) and Alzheimer's disease (**b**). The patient in **a** shows normal distribution of the tracer, whereas the patient with AD shows a high tracer uptake in the cortices of the frontal, temporal and occipital lobes consistent with a heavy amyloid burden

PCA has been developed, based on the degree of widening of the posterior cingulate, parietal and parieto-occipital sulci [41]. FDG-PET studies also demonstrate hypometabolism in these regions (Fig. 5) [42].

Vascular dementia

The notion of a potential link between dementia and compromised cerebral perfusion was first mentioned by

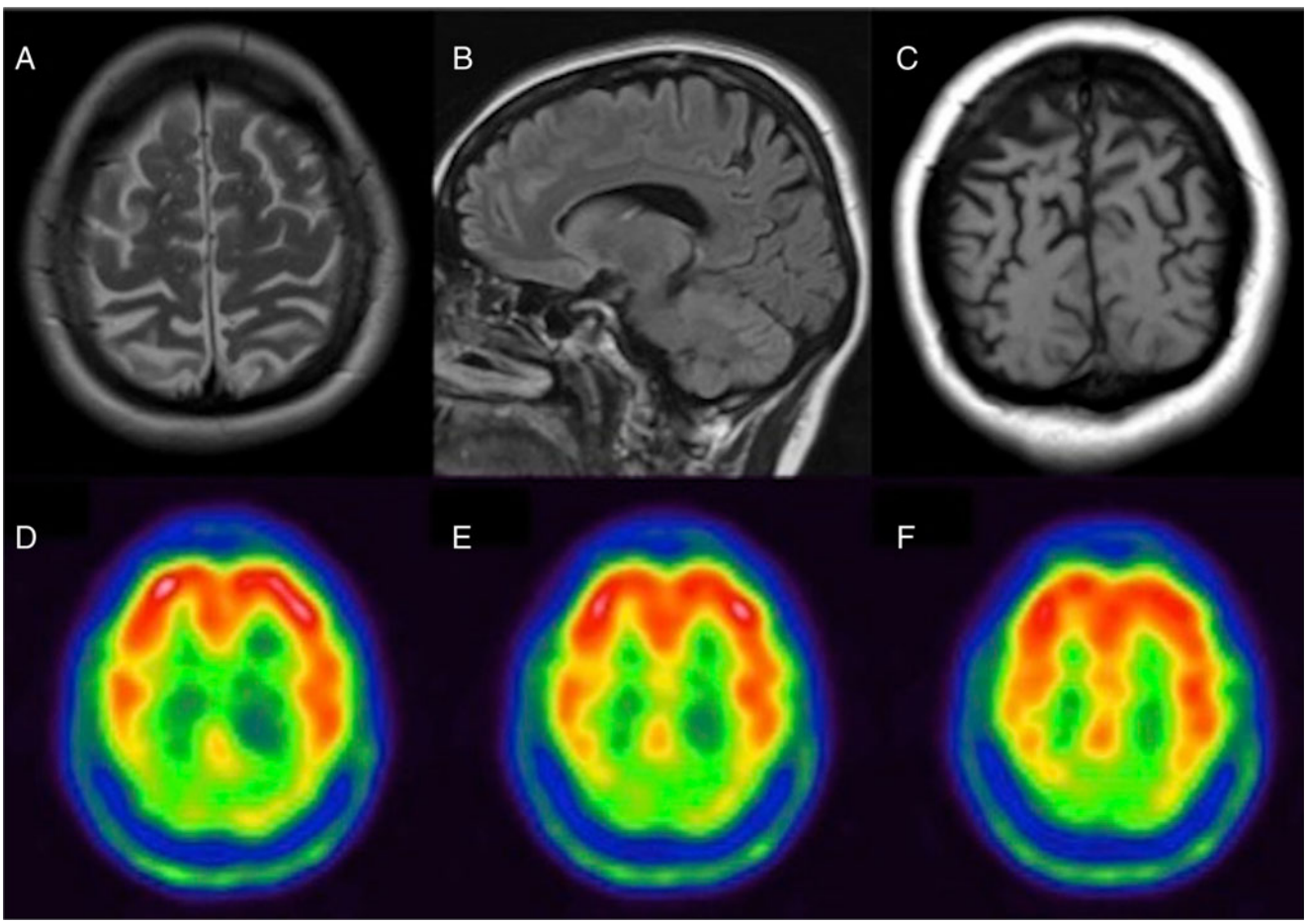

Fig. 5 A 55-year-old woman with posterior cortical atrophy (PCA). Axial T2 (**a**), sagittal FLAIR (**b**) and coronal T1-weighted (**c**) images demonstrate subtle enlargement of the inter-parietal, parieto-occipital and postcentral sulci . The FDG-PET CT (**d-f**) demonstrates marked hypometabolism in both parietal and occipital lobes and normal tracer uptake in the frontal lobes

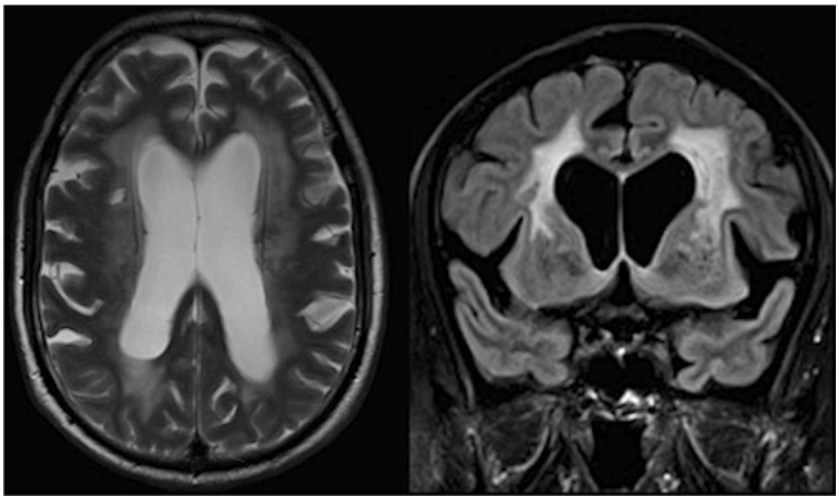

Fig. 6 Axial T2-weighted (**a**) and coronal FLAIR (**b**) images show extensive confluent hyperintense white matter lesions of presumed vascular origin, corresponding to Fazekas grade 3 small vessel disease. There is also predominantly central volume loss

Pratensis [43, 44]. Subsequently Alois Alzheimer and Otto Binswanger independently established a definite link between the two [43].

Today, vascular dementia (VaD) is the second most common cause of cognitive impairment after AD in the elderly [45], accounting for 20–40 % of cases [45–47]. Men are affected more frequently than women [48, 49] and a higher prevalence is seen in East Asia [49, 50]. Strong positive associations have also been demonstrated with age, low education level and vascular risk factors, including hypertension, diabetes mellitus, hyperlipidaemia and smoking [45].

It is increasingly recognised that VaD and AD interact and have additive effects [48]. Many of the predisposing cardiovascular risk factors associated with VaD are also linked to AD [44–52], and the co-existence of vascular and AD pathology is common with advancing age [51].

VaD may be caused by large or small vessel disease. Large vessel disease can cause single or multiple cortical and subcortical infarcts (Fig. 6) which may be associated with cognitive impairment, particularly if they involve strategic regions such as the hippocampus, thalamus, cingulate gyrus or angular gyrus.

An international workshop of the National Institute of Neurological Disorders and Stroke (NINDS) and the Association Internationale pour la Recherche et l'Enseignement en Neurosciences (AIREN) laid down criteria for VaD. The radiological component of the NINDS AIREN criteria show considerable interobserver variability and the operational definitions for these criteria improve the agreement for experienced observers [53].

Small vessel disease is the commonest cause of VaD. Imaging findings include focal and/or confluent white matter lesions, lacunes and small infarcts in the territory of the deep perforating vessels. The imaging manifestations of small vessel disease have recently been summarised in an excellent position paper aiming to provide Standards for Reporting Vascular changes on neuroimaging (STRIVE) [54].

A number of rating scales have been developed to describe the extent of white matter changes (WMC) in small vessel disease [1, 54]. The Fazekas scale , which uses four steps, is the simplest of these scales and can easily be used in clinical practice: 0=no WMC; 1=only punctate small WMC; 2=early confluent WMC; 3=confluent WMC. A score of 1 can be

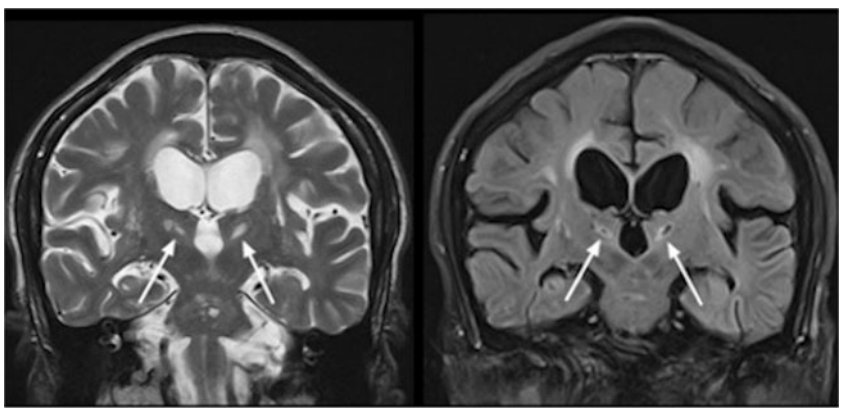

Fig. 7 Coronal T2-weighted and FLAIR images in a patient with small vessel disease and bilateral lacunes in the thalami. Confluent T2/FLAIR hyperintense signal in the periventricular white matter is typical for small vessel disease. The lacunes in the thalamus (*arrows*) appear bright on T2-weighted images but dark on the FLAIR images. Note also that the brainstem lesions are less well seen on FLAIR images

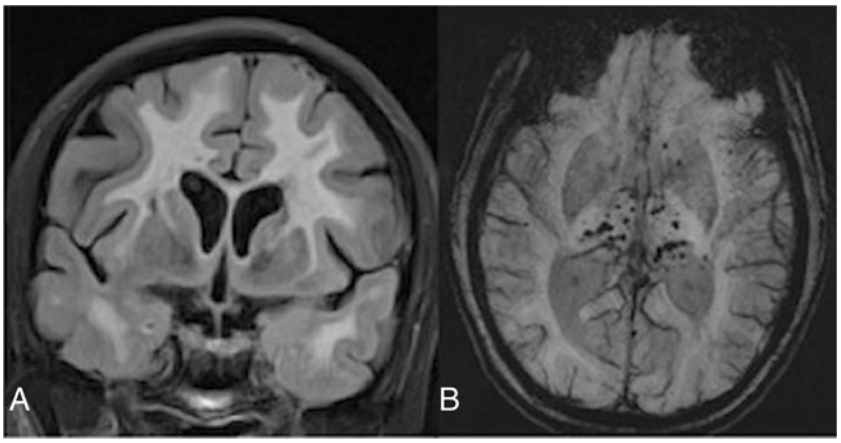

Fig. 8 A patient with proven CADASIL. Coronal FLAIR image (**a**) shows widespread and confluent white matter hyperintensities with involvement of the external capsules and temporal lobes bilaterally . The susceptibility-weighted (SWI) image shows multiple microhaemorrhages in both thalami, which is a typical location for CADASIL. The central location of microhaemorrhages is distinct from the peripheral distribution of these lesions seen in cerebral amyloid angiopathy and AD

considered normal above the age of 65 years, a score of 2 is abnormal below 70 years and a score of 3 is always abnormal.

VaD is most frequently seen with extensive confluent white matter lesions, multiple lacunes or bilateral small thalamic infarcts (Fig. 7). The clinical phenotypes of VaD are heterogeneous. Cortical infarcts may lead to aphasia, apraxia and seizures, whilst subcortical lesions are associated with executive dysfunction, gait disturbance, urinary incontinence, Parkinsonism and bradyphrenia [50, 52, 55].

In multi-infarct dementia (MID), large artery infarct episodes occur in close temporal relation to the onset of dementia [45]. Focal neurological signs occur with classically a stepwise progression of cognitive impairment [45]. In contrast, subcortical vascular dementia due to small vessel disease follows a more insidious course [45]. Depression occurs in up to 20 % of patiens with VaD, particularly with frontal white matter involvement [45, 56].

Whilst large cortical infarcts and extensive small vessel disease can readily be detected with CT, MRI is much more sensitive at detecting subtle white matter lesions [27] and smaller infarcts [1]. White matter lesions in small vessel disease appear hyperintense on T2 and FLAIR images and tend to spare the subcortical U fibres and temporal lobe, in contrast to multiple sclerosis [9]. Lacunes appear bright in T2-weighted images but dark on FLAIR images (Fig. 7).

Another advantage of MR imaging is that diffusion-weighted imaging (DWI) can identify acute infarcts and that T2*-weighted or susceptibility-weighted imaging enables the detection of cerebral microbleeds, which have an important association with cognitive impairment and an increased incidence in AD and cerebral amyloid angiopathy [57].

Compromise of cerebral blood flow in small or large vessel disease can be detected with MR perfusion imaging. A study using arterial spin-labelling (ASL) demonstrated that subjects with diffuse confluent white matter hyperintensities (WMH) have approximately 20 % lower cerebral blood flow (CBF) measurements than subjects with punctiform or early confluent WMH [58].

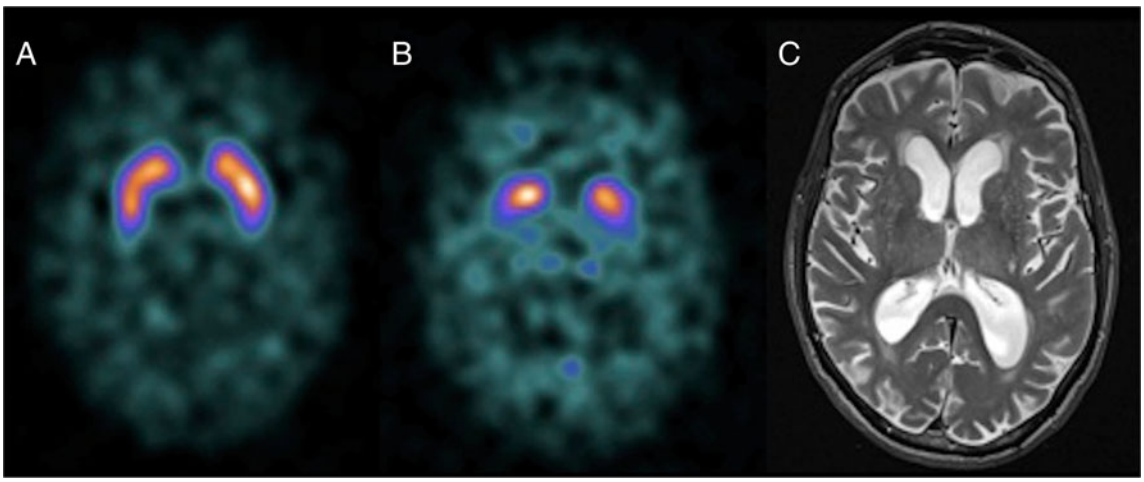

Fig. 9 Normal DAT scan (**a**) for comparison. DAT scan of a patient with DLB (**b**) showing lack of tracer uptake in the putamen bilaterally. Axial T2-weighted image (**c**) of the same patient shows non-specific generalised supratentorial volume loss

CADASIL (cerebral autosomal dominant arteriopathy with subcortical infarcts and leukoencephalopathy) is the most common genetic cerebrovascular disease and due to a mutation of the notch-3 gene [59]. Strokes usually occur in the 4th or 5th decade of life, with progression to a subcortical dementia. The radiological features of CADASIL are extensive white matter lesions with involvement of the temporal lobes and external capsules. Infratentorial and basal ganglia microbleeds are also a feature (Fig. 8).

Dementia with lewy bodies

Lewy bodies are intracellular pathological aggregations of alpha synuclein that were originally described in 1912 by Frederich Lewy. It is believed that dementia with Lewy bodies (DLB) accounts for between 15–20 % [60, 61] of dementia cases in the elderly. Clinically the diagnostic features are ranked as central, core, suggestive and supportive. The central feature required for the diagnosis is a progressive decline in cognition that is of sufficient magnitude to interfere with normal occupational or social function. Core features include fluctuating cognition with a decline in executive and visuoperceptual skills being common in addition to recurrent, well formed three-dimensional visual hallucinations and spontaneous features of Parkinsonism. Prominent episodic memory impairment is not uncommon and may mimic AD.

There is an overlap between DLB and Parkinson's disease, which can be regarded as ends of a continuous spectrum. Consensus agreement recommends that the diagnosis of DLB should be made if the dementia precedes the motor symptoms or has occurred within 12 months of the motor symptoms [62], whereas Parkinson's disease dementia (PDD) should be considered if motor features are present for at least 12 months before the onset of the dementia [63]. Differentiation of DLB from AD is important given the sensitivity of patients with DLB to neuroleptics. In contrast to AD, the memory impairment is often not as severe and visual hallucinations are more likely to occur in DLB.

Imaging findings of DLB are non-specific global and subcortical volume loss with relative preservation of the hippocampi, which can be a distinguishing feature from AD [64]. However, medial temporal lobe atrophy does not exclude DLB as it becomes more prominent with increasing age and severity.

Imaging of the dopaminergic pathway using single-photon emission computed tomography (SPECT) with the I^{123} presynaptic ligand, FP-CIT, has proven useful and is currently recommended by the National Institute for Health and Clinical Excellence (NICE) in the U.K. In normal healthy subjects and in patients with AD this ligand is readily taken up in both the caudate and putamen; however, in patients with DLB, uptake in the putamen is almost absent and in the caudate it is markedly reduced (Fig. 9). Several studies have shown that FP-CIT SPECT imaging has a sensitivity and specificity for DLB/PDD in the region of 80–90 % [65–67].

Cardiac sympathetic denervation, reflected by a decreased tracer uptake on iodine-123-metaiodobenzylguanidine (MIBG) myocardial scintigraphy has been detected in DLB but not in AD. This technique has been shown to have a 98 % sensitivity of differentiating DLB from other dementias [68] and is currently part of the latest guidelines as one of the supportive features for diagnosing DLB.

Frontotemporal lobar degeneration

Frontotemporal lobar degeneration (FTLD) refers to the pathological entities that underlie a number of clinical syndromes often with focal cortical atrophy. It is estimated to be the third most common cause of primary dementia [69], and the second most common cause of early-onset dementia. Broadly speaking two main sub-types exist: a behavioural-led syndrome (bvFTD) and a language-led syndrome (primary progressive aphasia [PPA]) (Fig. 10).

BvFTD is a clinical syndrome characterised by progressive deterioration in social cognition. Common early features may include combinations of behavioural disinhibition, apathy, loss of empathy, compulsive behaviour and hyperorality [70].

PPA encompasses three distinct clinical subtypes:

1. Semantic variant PPA (sv-PPA), characterised by fluent speech, anomia and loss of object knowledge
2. Non-fluent/agrammatic PPA (nv-PPA), characterised by effortful speech production and orofacial apraxia
3. Logopenic variant PPA (lv-PPA) characterised by word-finding pauses and poor sentence repetition [71]

With the advent of modern immunohistochemistry, the protein basis for these diseases have become clearer. BvFTD is most commonly associated with tau or TDP-43 protein deposition; sv-PPA most commonly with TDP-43 and nv-PPA with tau and to a lesser degree TDP-43. AD pathology is found commonly in those with lv-PPA and occasionally in cases of nv-PPA [72, 73]. In a significant proportion of these cases a movement disorder will also emerge (Fig. 10) [74].

Structural neuroimaging, preferably with MRI, is an essential part of the evaluation of suspected FTLD. The classical description of FTLD is atrophy of the frontal and temporal cortices, which is often asymmetrical, with relative sparing of the parietal and occipital lobes [75].

Characteristic patterns of atrophy have been described for each of the clinical subtypes of FTLD.

Typically bvFTD shows symmetrical frontal lobe atrophy (Fig. 11), although asymmetric patterns of atrophy predominantly involving the right frontal [76] and/or right temporal lobe [75] can occur (Fig. 12).

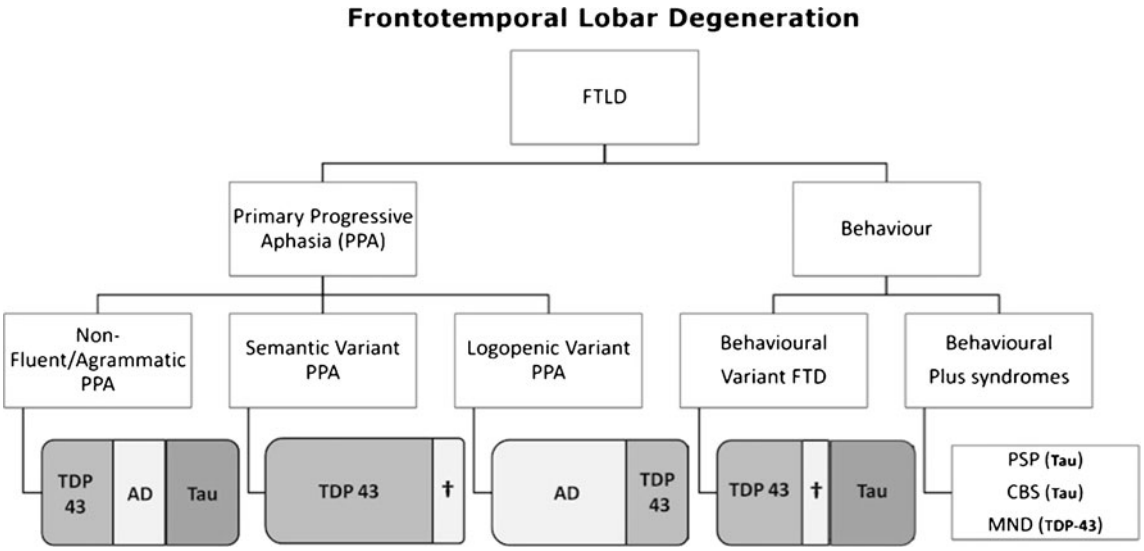

Fig. 10 Schematic diagram of FTLD subtypes, separating those with a behaviour-led presentation from those with a language-led clinical presentation. The *bottom line* of the diagram indicates the common pathological findings associated with these clinical presentations

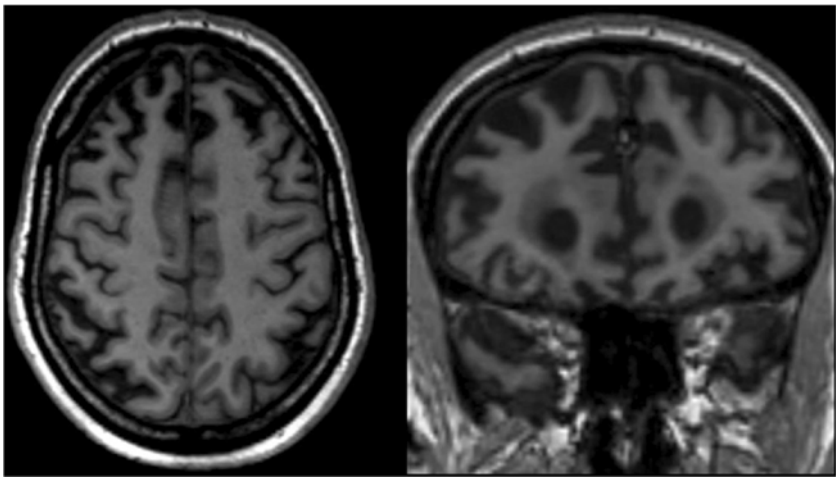

Fig. 11 Axial (**a**) and coronal (**b**) volumetric T1 weighted images in a patient with bvFLT showing marked symmetrical volume loss in the frontal lobes with a "knife edge" appearance of the superior and middle frontal gyri

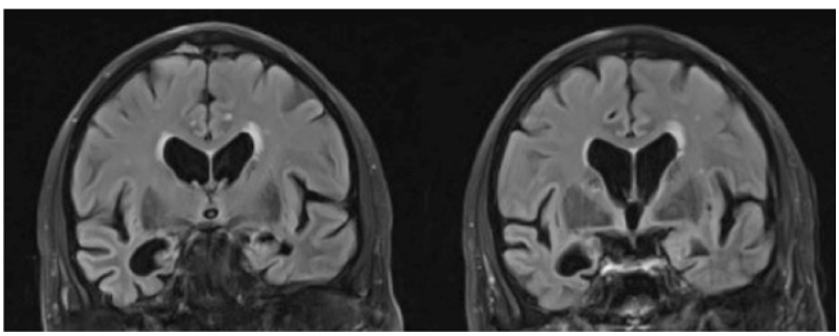

Fig. 12 Coronal FLAIR images in a patient with a right temporal variant of bvFTD . There is marked asymmetrical volume loss of the right temporal lobe affecting all the temporal gyri and resulting in marked dilatation of the right temporal horn. There is much less marked atrophy of the left temporal lobe and dilatation of both lateral ventricles

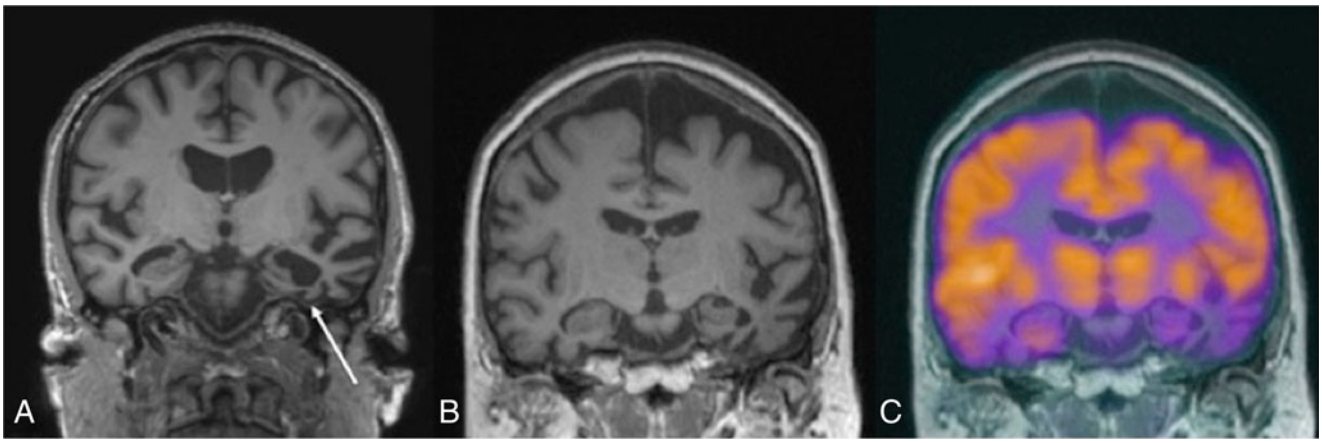

Fig. 13 Coronal T1-weighted images (**a**, **b**) and fused FDG PET MRI image (**c**) in a patient with sematic variant PPA (semantic dementia). **a**, **b** Marked asymmetrical volume loss is found in the left temporal lobe affecting all temporal gyri and particularly the fusiform gyrus (*arrow*). **c** The FDG PET MRI demonstrates glucose hypometabolism not only in the left but also in the right temporal lobe, which shows much less marked atrophy

In contrast, patients with the language variants often demonstrate left-sided asymmetric volume loss. In semantic variant PPA, there is typically atrophy in the left anterior inferior temporal lobe (with "knife-edge"–type gyri) affecting particularly the fusiform gyrus but the entire left temporal lobe can be involved (Fig. 13) [77, 78]. In addition, there is often involvement of the ventromedial and superior frontal lobes and, as the disease progresses, the right temporal lobe can also show a less marked degree of volume loss.

The findings in non-fluent/agrammatic PPA are of selective left perisylvian and frontal atrophy. In logopenic variant PPA, the atrophy is mainly left-sided and more posterior, involving the angular and middle temporal gyri (Fig. 14) [68, 71].

Unlike AD, up to 40 % of individuals with FTLD will have a genetic explanation for their syndrome [74]. A number of autosomal dominant mutations have been described with particular patterns of brain atrophy. Focal medial temporal lobe atrophy with parahippocampal and bilateral anterior-inferior temporal lobe atrophy is seen in microtubule-associated tau protein (MAPT) mutations. Highly asymmetric hemispheric atrophy has been associated with mutations in the progranulin gene (GRN) (Fig. 15) [69]. More recently, a major new mutation has been identified as a cause of FTLD and motor neurone disease (C9ORF72 gene expansion) showing a heterogeneous but predominantly symmetrical pattern of atrophy [79].

Quantitative MRI studies, using automated image analysis techniques, have refined these visual observations, with particular patterns of atrophy having a strong predictive value for particular underlying pathologies [80, 81]. These techniques are not routinely available in a clinical setting at present and, as for AD and PCA, visual rating scales for clinical use have also been developed for frontotemporal dementia [78].

FDG-PET and amyloid PET help to differentiate FTLD from AD [82, 83]. FTLD is not associated with increased

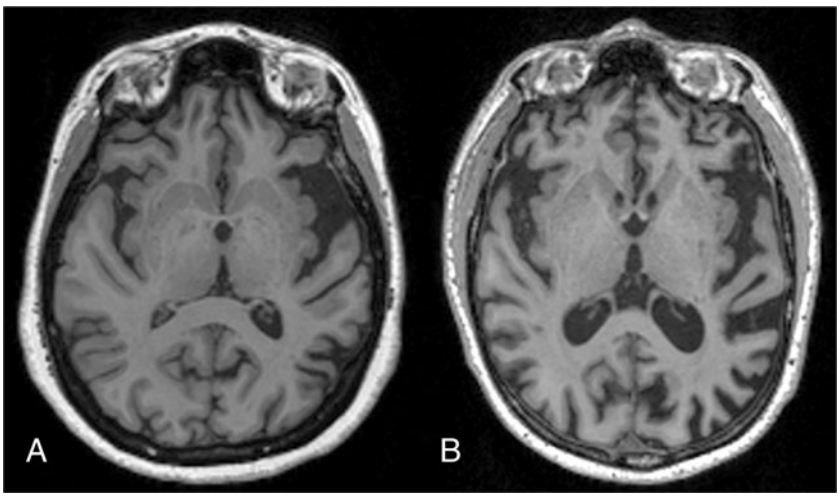

Fig. 14 Axial T1-weighted MRI images in two different types of language led FLTD: non-fluent/agrammatic PPA (**a**) and logopenic variant PPA (**b**). Both cases show a markedly asymmetrical atrophy affecting predominantly the left hemisphere. In non-fluent/agrammatic PPA, the volume loss is centred around the left perisylvian region with resulting enlargement of the left Sylvian fissure (**a**). In the logopenic variant PPA, there is much more marked involvement of the left angular gyrus and posterior temporal lobe as well as occipital lobe (**b**)

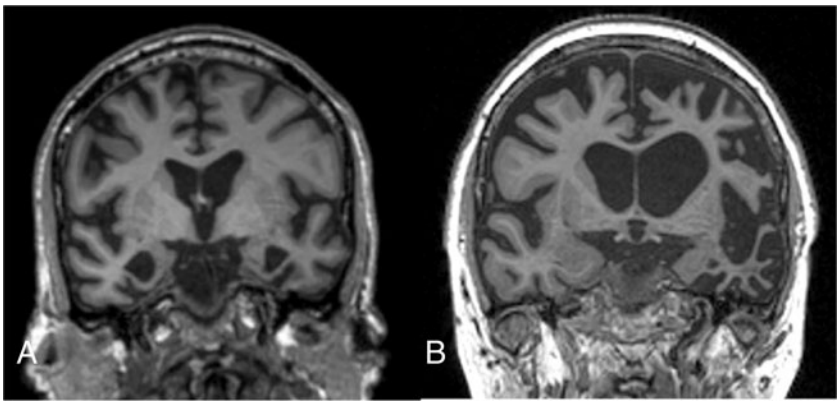

Fig. 15 Coronal T1-weighted images of two different cases of autosomal dominant FTLD: microtubule associated tau protein (MAPT) mutation (**a**) and mutation of the progranulin gene (**b**). The MAPT mutation (**a**) shows symmetrical atrophy of the medial temporal lobes with characteristic "ballooning" of the temporal horn of the lateral ventricles. The progranulin mutation (**b**) showed markedly asymmetric atrophy with "knife edge" appearance of the left temporal and frontal gyri, and marked expansion of the left lateral ventricle and Sylvian fissure

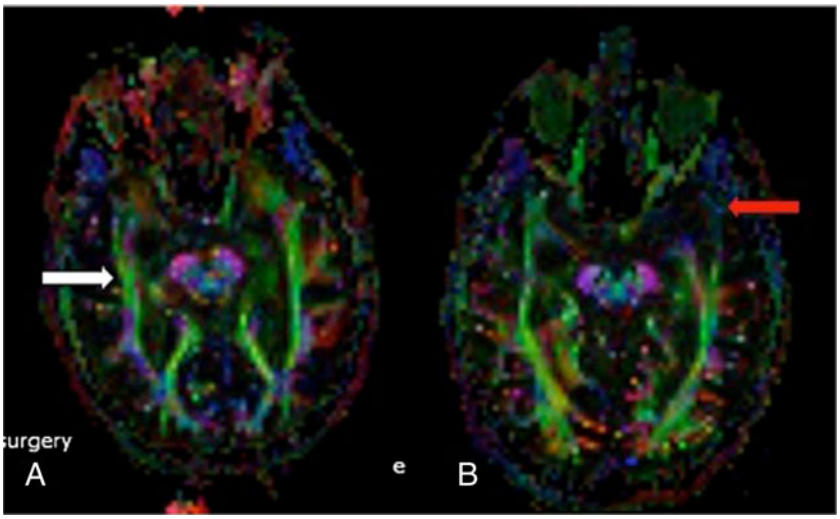

Fig. 16 Diffusion tensor imaging (DTI) with two different cases of FTLD: right temporal lobe bvFTD (**a**) and semantic variant PPA (**b**) showing asymmetry of the inferior longitudinal fasciculi (ILF), which are major association fibres connecting the temporal and occipital lobes. In **a** there is atrophy of the right ILF (*white arrow*) and in **b** there is atrophy of the left ILF (*red arrow*)

amyloid burden and shows distinct patterns of hypometabolism in specific clinical syndromes, with frontal hypometabolism being associated with bvFTD, temporal with sv-PPA and left perisylvian with nv-PPA [83, 84].

Diffusion tensor imaging (DTI) can demonstrate involvement of specific white matter tracts in various subtypes of FTLD (Fig. 16).

There are fewer DTI studies of white matter alterations in bvFTD than AD. Widespread changes in white matter have been reported, with a particular emphasis on anterior tracts including the uncinate fasciculus, inferior longitudinal fasciculus and anterior commissural fibres [85]. PPA damage to the following tracts has been reported: inferior longitudinal fasciculus and uncinate fasciculus in sv-PPA; left superior longitudinal fasciculus and anterior thalamic radiations in nv-PPA and widespread dorsal and ventral white matter tracts in lv-PPA [86, 87]. There have been few fMRI studies in bvFTD, although one major study examining resting state activity identified reduced activity within a 'Salience Network', an area overlapping the anterior cingulate and frontoinsular cortices, an important brain region for the interpretation of social cognition [88]. One task-based fMRI study using non-verbal sounds identified different patterns of brain activation within the superior temporal cortex in sv-PPA when compared with healthy individuals.

Conclusions

The role of neuroimaging in dementia has changed in the past decade; it is no longer merely performed as a means to exclude underlying conditions such as brain tumours or infarcts. MR imaging, especially volumetric T1-weighted images, can

show specific patterns of focal atrophy which have a high positive predictive value for a number of dementia subtypes. It is important for radiologists to be aware of the typical imaging appearances of the common causes of dementia. In addition, functional and molecular imaging techniques can improve the diagnostic accuracy and help early disease detection.

References

1. Barkhof F, Fox NC, Bastos-Leite AJ, Scheltens P (2011) Neuroimaging in dementia. Springer, Heidelberg, pp 62–66
2. Farlow M (2007) Alzheimer's disease. Continuum Lifelong Learn Neurol 13:39–68
3. Terry RD, Peck A, DeTeresa R, Schechter R, Horoupian DS (1981) Some morphometric aspects of the brain in senile dementia of the Alzheimer type. Ann Neurol 10:184–192
4. Terry RD, Masliah E, Salmon DP et al (1991) Physical basis of cognitive alterations in Alzheimer's disease: synapse loss is the major correlate of cognitive impairment. Ann Neurol 30:572–580
5. Braak H, Braak E (1994) Morphological criteria for the recognition of Alzheimer's disease and the distribution pattern of cortical changes related to this disorder. Neurobiol Aging 15:355–356, discussion 79–80
6. Tomlinson BE, Blessed G, Roth M (1970) Observations on the brains of demented old people. J Neurol Sci 11:205–242
7. Farias ST, Mungas D, Reed BR, Harvey D, DeCarli C (2009) Progression of mild cognitive impairment to dementia in clinic- vs community-based cohorts. Arch Neurol 66:1151–1157
8. Jack CR Jr, Weigand SD, Shiung MM et al (2008) Atrophy rates accelerate in amnestic mild cognitive impairment. Neurology 70: 1740–1752
9. McKhann GM, Knopman DS, Chertkow H et al (2011) The diagnosis of dementia due to Alzheimer's disease: recommendations from the National Institute on Aging-Alzheimer's Association workgroups on diagnostic guidelines for Alzheimer's disease. Alzheimers Dement 7:263–269
10. Jack CR Jr (2012) Alzheimer disease: new concepts on its neurobiology and the clinical role imaging will play. Radiology 263:344–361
11. Jack CR Jr, Knopman DS, Jagust WJ et al (2010) Hypothetical model of dynamic biomarkers of the Alzheimer's pathological cascade. Lancet Neurol 9:119–128
12. Qiu C, Kivipelto M, von Strauss E (2009) Epidemiology of Alzheimer's disease: occurrence, determinants and strategies toward intervention. Dialogues Clin Neurosci 11:111–128
13. Janssen JC, Beck JA, Campbell TA et al (2003) Early onset familial Alzheimer's disease: mutation frequency in 31 families. Neurology 60:235–239
14. St George-Hyslop PH, Tanzi RE, Polinsky RJ et al (1987) The genetic defect causing familial Alzheimer's disease maps on chromosome 21. Science 235:885–890
15. Davies P (1986) The genetics of Alzheimer's disease: a review and a discussion of the implications. Neurobiol Aging 7:459–466
16. Goate A, Chartier-Harlin MC, Mullan M et al (1991) Segregation of a missense mutation in the amyloid precursor protein gene with familial Alzheimer's disease. Nature 349:704–706
17. Levy-Lahad E, Wasco W, Poorkaj P et al (1995) Candidate gene for the chromosome 1 familial Alzheimer's disease locus. Science 269:973–977
18. Sherrington R, Rogaev EI, Liang Y et al (1995) Cloning of a gene bearing missense mutations in early-onset familial Alzheimer's disease. Nature 375:754–760
19. Scheuner D, Eckman C, Jensen M et al (1996) Secreted amyloid beta-protein similar to that in the senile plaques of Alzheimer's disease is increased in vivo by the presenilin 1 and 2 and APP mutations linked to familial Alzheimer's disease. Nature Med 2:864–780
20. Cavedo E, Boccardi M, Ganzola R et al (2011) Local amygdala structural differences with 3T MRI in patients with Alzheimer disease. Neurology 22:727–733
21. Jack CR Jr, Shiung MM, Gunter JL et al (2004) Comparison of different MRI brain atrophy rate measures with clinical disease progression in AD. Neurology 62:591–600
22. Jack CR Jr, Petersen RC, Xu Y et al (1998) Rate of medial temporal lobe atrophy in typical aging and Alzheimer's disease. Neurology 51: 993–999
23. De Leon MJ, George AE, Golomb J et al (1997) Frequency of hippocampal formation atrophy in normal aging and Alzheimer's disease. Neurobiol Aging 18:1–11
24. de Toledo-Morrell L, Dickerson B, Sullivan MP, Spanovic C, Wilson R, Bennett DA (2000) Hemispheric differences in hippocampal volume predict verbal and spatial memory performance in patients with Alzheimer's disease. Hippocampus 10:136–142
25. Uotani C, Sugimori K, Kobayashi K (2006) Association of minimal thickness of the medial temporal lobe with hippocampal volume, maximal and minimal hippocampal length: volumetric approach with horizontal magnetic resonance imaging scans for evaluation of a diagnostic marker for neuroimaging of Alzheimer's disease. Psychiatry Clin Neurosci 60:319–326
26. Scheltens P, Launer LJ, Barkhof F, Weinstein HC, van Gool WA (1995) Visual assessment of medial temporal lobe atrophy on magnetic resonance imaging: interobserver reliability. J Neurol 242:557–560
27. Wattjes MP, Henneman WJ, van der Flier WM et al (2009) Diagnostic imaging of patients in a memory clinic: comparison of MR imaging and 64-detector row CT. Radiology 253:174–183
28. Leung KK, Clarkson MJ, Bartlett JW, Clegg S, Jack CR Jr, Weiner MW, Fox NC, Ourselin S (2010) Robust atrophy rate measurement in Alzheimer's disease using multi-site serial MRI: tissue-specific intensity normalization and parameter selection. Neuroimage 50:516–523
29. Klunk WE, Engler H, Nordberg A et al (2004) Imaging brain amyloid in Alzheimer's disease with Pittsburgh Compound-B. Ann Neurol 55:306–319
30. Mathis CA, Kuller LH, Klunk WE et al (2013) In vivo assessment of amyloid-beta deposition in nondemented very elderly subjects. Ann Neurol 76:751–761
31. Musiek ES, Chen Y, Korczykowski M et al (2012) Direct comparison of fluorodeoxyglucose positron emission tomography and arterial spin labeling magnetic resonance imaging in Alzheimer's disease. Alzheimers Dement 8:51–59
32. Yoshiura T, Hiwatashi A, Noguchi T et al (2009) Arterial spin labelling at 3-T MR imaging for detection of individuals with Alzheimer's disease. Eur Radiol 19:2819–2825
33. Sexton CE, Kalu UG, Filippini N, Mackay CE, Ebmeier KP (2011) A meta-analysis of diffusion tensor imaging in mild cognitive impairment and Alzheimer's disease. Neurobiol Aging 32:5–18
34. Mielke MM, Kozauer NA, Chan KC et al (2009) Regionally-specific diffusion tensor imaging in mild cognitive impairment and Alzheimer's disease. Neuroimage 46:47–55
35. Greicius MD, Srivastava G, Reiss AL, Menon V (2004) Default-mode network activity distinguishes Alzheimer's disease from healthy aging: evidence from functional MRI. Proc Natl Acad Sci U S A 101:4637–4642
36. Filippini N, MacIntosh BJ, Hough MG et al (2009) Distinct patterns of brain activity in young carriers of the APOE-epsilon4 allele. Proc Natl Acad Sci U S A 106:7209–7214
37. Renner JA, Burns JM, Hou CE, McKeel DW Jr, Storandt M, Morris JC (2004) Progressive posterior cortical dysfunction: a clinicopathologic series. Neurology 63:1175–1180
38. Tang-Wai DF, Graff-Radford NR, Boeve BF et al (2004) Clinical, genetic, and neuropathologic characteristics of posterior cortical atrophy. Neurology 63:1168–1174

39. Lehmann M, Crutch SJ, Ridgway GR et al (2011) Cortical thickness and voxel-based morphometry in posterior cortical atrophy and typical Alzheimer's disease. Neurobiol Aging 32:1466–1476
40. Whitwell JL, Jack CR Jr, Kantarci K et al (2007) Imaging correlates of posterior cortical atrophy. Neurobiol Aging 28:1051–1061
41. Koedam ELGE, Lehmann M, van der Flier WM et al (2011) Visual assessment of posterior atrophy development of a MRI rating scale. Eur Radiol 21:2618–2625
42. Wakai M, Honda H, Takahashi A, Kato T, Ito K, Hamanaka T (1994) Unusual findings on PET study of a patient with posterior cortical atrophy. Acta Neurol Scand 89:458–461
43. Iemolo F, Duro G, Rizzo C, Castiglia L, Hachinski V, Caruso C (2009) Pathophysiology of vascular dementia. Immun Ageing 6:13
44. Enciu AM, Constantinescu SN, Popescu LM, Muresanu DF, Popescu BO (2011) Neurobiology of vascular dementia. J Aging Res 2011: 401604
45. Lee AY (2011) Vascular dementia. Chonnam Med J 47:66–71
46. Fratiglioni L, Rocca WA (2001) Epidemiology of dementia. In: Boller F, Cappa SF (eds) Handbook of neuropsychology, 2nd edn. Elsevier, Amsterdam, pp 193–215
47. O'Brien JT, Erkinjuntti T, Reisberg B et al (2003) Vascular cognitive impairment. Lancet Neurol 2:89–98
48. Leys D, Henon H, Mackowiak-Cordoliani MA, Pasquier F (2005) Poststroke dementia. Lancet Neurol 4:752–759
49. Korczyn AD, Vakhapova V, Grinberg LT (2012) Vascular dementia. J Neurol Sci 322:2–10
50. Ikeda M, Hokoishi K, Maki N et al (2001) Increased prevalence of vascular dementia in Japan: a community-based epidemiological study. Neurology 57:839–844
51. Skoog I, Korczyn AD, Guekht A (2012) Neuroprotection in vascular dementia: a future path. J Neurol Sci 322:232–236
52. Koga H, Takashima Y, Murakawa R, Uchino A, Yuzuriha T, Yao H (2009) Cognitive consequences of multiple lacunes and leukoaraiosis as vascular cognitive impairment in community-dwelling elderly individuals. J Stroke Cerebrovasc Dis 18:32–37
53. van Straaten EC, Scheltens P, Knol DL, van Buchem MA, van Dijk EJ, Hofman PA et al (2003) Operational definitions for NINDS-AIREN criteria for vascular dementia. An interobserver study. Stroke 34:1907–1912
54. Wardlaw JM, Smith EE, Biessels GJ et al (2013) Neuroimaging standards for research into small vessel disease and its contribution to ageing and neurodegeneration. STandards for ReportIng Vascular changes on nEuroimaging (STRIVE v1). Lancet Neurol 12:822–838
55. Handley A, Medcalf P, Hellier K, Dutta D (2009) Movement disorders after stroke. Age Ageing 38:260–266
56. Udaka F, Sawada H, Kameyama M (2002) White matter lesions and dementia: MRI-pathological correlation. Ann N Y Acad Sci 977: 411–415
57. Charidimou A, Werring DJ (2012) Cerebral microbleeds and cognition in cerebrovascular disease: an update. J Neurol Sci 322:50–55
58. Bastos-Leite AJ, Kuijer JP, Rombouts SA et al (2008) Cerebral blood flow by using pulsed arterial spin-labeling in elderly subjects with white matter hyperintensities. AJNR Am J Neuroradiol 29:1296–1301
59. Chabriat H, Joutel A, Dichgans M, Tournier-Lasserve E, Bousser MG (2009) Cadasil. Lancet Neurol 8:643–653
60. Hansen L, Salmon D, Galasko D et al (1990) The Lewy body variant of Alzheimer's disease: a clinical and pathologic entity. Neurology 40:1–8
61. Perry RH, Irving D, Blessed G, Fairbairn A, Perry EK (1990) Senile dementia of Lewy body type. A clinically and neuropathologically distinct form of Lewy body dementia in the elderly. J Neurol Sci 95: 119–139
62. McKeith IG, Dickson DW, Lowe J et al (2005) Diagnosis and management of dementia with Lewy bodies: third report of the DLB Consortium. Neurology 65:1863–1872
63. Emre M, Aarsland D, Brown R et al (2007) Clinical diagnostic criteria for dementia associated with Parkinson's disease. Mov Disord 22:1689–1707, quiz 837
64. Burton EJ, Karas G, Paling SM et al (2002) Patterns of cerebral atrophy in dementia with Lewy bodies using voxel-based morphometry. Neuroimage 17:618–630
65. Marshall VL, Patterson J, Hadley DM, Grosset KA, Grosset DG (2006) Two-year follow-up in 150 consecutive cases with normal dopamine transporter imaging. Nucl Med Commun 27:933–937
66. McKeith I, O'Brien J, Walker Z et al (2007) Sensitivity and specificity of dopamine transporter imaging with 123I-FP-CIT SPECT in dementia with Lewy bodies: a phase III, multicentre study. Lancet Neurol 6:305–313
67. Walker Z, Jaros E, Walker RW et al (2007) Dementia with Lewy bodies: a comparison of clinical diagnosis, FP-CIT single photon emission computed tomography imaging and autopsy. J Neurol Neurosurg Psychiatry 78:1176–1181
68. Treglia G, Cason E (2012) Diagnostic performance of myocardial innervation imaging using MIBG scintigraphy in differential diagnosis between dementia with Lewy bodies and other dementias: a systematic review and a meta-analysis. J Neuroimaging 22:111–117
69. Gallucci M, Limbucci N, Catalucci A, Caulo M (2008) Neurodegenerative diseases. Radiol Clin North Am 46:799–817, vii
70. Seelaar H, Rohrer JD, Pijnenburg YA, Fox NC, van Swieten JC (2011) Clinical, genetic and pathological heterogeneity of frontotemporal dementia: a review. J Neurol Neurosurg Psychiatry 82:476–486
71. Gorno-Tempini ML, Dronkers NF, Rankin KP et al (2004) Cognition and anatomy in three variants of primary progressive aphasia. Ann Neurol 55:335–346
72. Seelaar H, Kamphorst W, Rosso SM et al (2008) Distinct genetic forms of frontotemporal dementia. Neurology 71:1220–1226
73. Cairns NJ, Bigio EH, Mackenzie IR et al (2007) Neuropathologic diagnostic and nosologic criteria for frontotemporal lobar degeneration: consensus of the Consortium for Frontotemporal Lobar Degeneration. Acta Neuropathol 114:5–22
74. Rohrer JD, Lashley T, Schott JM et al (2011) Clinical and neuroanatomical signatures of tissue pathology in frontotemporal lobar degeneration. Brain 134:2565–2581
75. Josephs KA (2007) Frontotemporal lobar degeneration. Neurol Clin 25:683–696, vi
76. Fukui T, Kertesz A (2000) Volumetric study of lobar atrophy in Pick complex and Alzheimer's disease. J Neurol Sci 174:111–121
77. Chan D, Fox NC, Scahill RI et al (2001) Patterns of temporal lobe atrophy in semantic dementia and Alzheimer's disease. Ann Neurol 49:433–442
78. Kipps CM, Davies RR, Mitchell J et al (2007) Clinical significance of lobar atrophy in frontotemporal dementia: application of an MRI visual rating scale. Dement Geriatr Cogn Disord 23:334–342
79. Mahoney CJ, Beck J, Rohrer JD et al (2012) Frontotemporal dementia with the C9ORF72 hexanucleotide repeat expansion: clinical, neuroanatomical and neuropathological features. Brain 135:736–750
80. Rosen HJ, Gorno-Tempini ML, Goldman WP et al (2002) Patterns of brain atrophy in frontotemporal dementia and semantic dementia. Neurology 58:198–208
81. Du AT, Schuff N, Kramer JH et al (2007) Different regional patterns of cortical thinning in Alzheimer's disease and frontotemporal dementia. Brain 130:1159–1166
82. Foster NL, Heidebrink JL, Clark CM et al (2007) FDG-PET improves accuracy in distinguishing frontotemporal dementia and Alzheimer's disease. Brain 130:2616–2635
83. Vitali P, Migliaccio R, Agosta F et al (2008) Neuroimaging in dementia. Semin Neurol 28:467–483
84. Diehl-Schmid J, Grimmer T, Drzezga A et al (2007) Decline of cerebral glucose metabolism in frontotemporal dementia: a longitudinal 18F-FDG-PET-study. Neurobiol Aging 28:42–50

85. Zhang Y, Schuff N, Du AT et al (2009) White matter damage in frontotemporal dementia and Alzheimer's disease measured by diffusion MRI. Brain 132:2579–2592
86. Mahoney CJ, Malone IB, Ridgway GR et al (2013) White matter tract signatures of the progressive aphasias. Neurobiol Aging 34: 1687–1699
87. Galantucci S, Tartaglia MC, Wilson SM et al (2011) White matter damage in primary progressive aphasias: a diffusion tensor tractography study. Brain 134:3011–3029
88. Zhou J, Greicius MD, Gennatas ED et al (2010) Divergent network connectivity changes in behavioural variant frontotemporal dementia and Alzheimer's disease. Brain 133:1352–1367

Editor's note

Readers will notice that this issue contains two rather similar review articles on the imaging of dementia. Both articles try to help the average radiologist identify key features which may require expert neuroradiological attention. Two groups spontaneously submitted a review article at roughly the same time. There were merits in both papers; both were favourably reviewed. It was an impossible editorial choice to select one paper over another and hence both are published alongside each other. It will be interesting to see whether the astute readers will identify differences. Indeed this may lead to some interesting discussion in the opinion column on the journal's website.